Random quasi-phase-matching in a nonlinear photonic crystal structure of strontium tetraborate

A. S. Aleksandrovsky* and A. M. Vyunishev

*L.V. Kirensky Institute of Physics, Akademgorodok, Krasnoyarsk 660036, Russia and Siberian Federal University,
Krasnoyarsk 660079, Russia*

I. E. Shakhura

Siberian Federal University, Krasnoyarsk 660079, Russia

A. I. Zaitsev

*L.V. Kirensky Institute of Physics, Akademgorodok, Krasnoyarsk 660036, Russia and Siberian Federal University,
Svobodnii, 79, Krasnoyarsk 660079, Russia*

A. V. Zamkov

L.V. Kirensky Institute of Physics, Akademgorodok, Krasnoyarsk 660036, Russia

Random quasi-phase-matching (RQPM) of the second-harmonic generation process is investigated experimentally and theoretically in a strongly randomized spontaneously grown nonlinear photonic crystal structure of strontium tetraborate. The thickness of domains in the structure is measured and employed in calculations of angular and spectral dependences of random quasi-phase-matching. Despite the great scale of randomness, the RQPM effect is preserved. The calculated enhancement factor due to RQPM is in excellent agreement with experiment, and good agreement between calculations and experiment is obtained for the shape of the angular dependence of RQPM. The calculated spectral dependence of RQPM consists of a number of narrow peaks, and a maximum enhancement factor is attained in the near ultraviolet. The band structure of randomized nonlinear photonic crystal is calculated.

Nonlinear optical media with spatially modulated susceptibility of second order have been known to increase the outcome of nonlinear optical processes since 1962 [1]. Berger [2] suggested classifying these media as nonlinear photonic crystals in analogy with linear photonic crystals that possess spatial modulation of the linear refractive index. Tailored periodically poled nonlinear crystal superlattices (NCSs) open up possibilities in the generation of entangled photon states [3,4]. A special case of NCSs is random nonlinear media with quasiperiodical modulation of nonlinear susceptibility. These media exhibit the phenomenon of random quasi-phase-matching (RQPM) [5,6]. A nonlinearly optically generated wave in randomized NCSs does not oscillate between zero and the maximum attained at the coherence length, but generally speaking, its intensity linearly increases with the length of the NCSs [7]. Modeling of random nonlinear media may give certain randomized structures with nearly zero outcome due to the destructive interference between radiation generated by all oppositely poled domains. However, under certain restrictions applied to the degree of randomness, the average over a sufficiently large number of possible random geometries gives a gradual increase of the outcome intensity with the number of domains. In other representations, the spectrum of reciprocal superlattice vectors (RSVs) must contain a vector with a length suitable to compensate for the wave-vector mismatch [8]. Nonlinear optical studies of NCSs can reveal the degree of

quasiperiodicity and examine the RSV spectrum [8–10]. Along with collinear nonlinear processes, NCSs demonstrate also noncollinear phase-matched conversion of radiation (see, e.g., [11] for strontium barium nobiate (SBN) crystal, [12] for rubidium dihydrophosphate (RDP), [10] for strontium tetraborate (SBO), and [13] for lithium niobate; earlier references concerning nonlinear diffraction can be found in [10]).

Materials commonly used for experiments with alternate oppositely poled nonlinear crystals are either ferroelectrics with the desired geometry of domains produced with a suitable poling procedure or polycrystalline samples with a random orientation of grains. A recent study revealed the existence of alternate oppositely poled domains in SBO [10,14]. SBO possesses transparency in the vacuum ultraviolet that enabled nonlinear optical generation of radiation at a wavelength as short as 125 nm [15]. However, birefringence of SBO is too small to achieve angular phase matching. Presently this crystal is not known to be a ferroelectric, and the mechanism of formation of alternate oppositely poled domain structures is unclear. The procedure for the production of regular domain structure is not developed. As-grown domain structures in SBO are shown to be well ordered along the directions of the b and c crystallographic axes, but they are highly randomized along the direction of the a axis. Domains have the form of sheets with domain walls perpendicular to the a axis. This geometry of domains is identical to potassium titanyl phosphate crystal, which belongs to the same point symmetry group $mm2$ as SBO. Evidently, these domain structures must exhibit the RQPM effect. In the present study we report SHG enhancement due to RQPM in
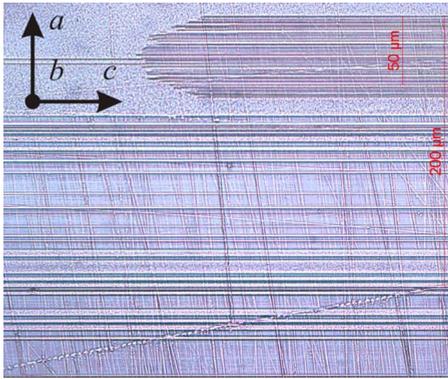
_____
*aleksandrovsky@kirensky.ru

FIG. 1. (Color online) Photo of a part of the domain structure on the (001) surface of strontium tetraborate crystal after etching.

SBO and demonstrate good agreement of experimental results with calculations based on the model outlined in [7].

When the geometry of a certain randomized domain structure dictates destructive interference of radiation from all domains, this interference condition must not be simultaneously fulfilled for all wavelengths of fundamental radiation and for all directions inside the crystal. When the fundamental wave propagates at nonzero angle to the domain walls, the RSV spectrum in a coordinate system of light beams experiences a shift and stretching. At certain angles RQPM conditions may become more favorable. For any real geometry the effect can be calculated using the approach developed in [6,7]. In the plane-wave approximation the amplitude of the generated field is a sum of those generated by separate domains, with account of the phase acquired while propagating to the detection plane. The formula modified for our case looks like

$$E_{2\omega} = \sum_{n=1}^{N} \left\{ \frac{2\omega^2 \chi_n^{(2)}}{k_{2\omega}(\theta_{int}) \Delta k(\theta_{int})} E_{\omega}^2 \left[\exp\left(i\Delta k(\theta_{int}) \frac{d_n}{\cos(\theta_{int})} \right) - 1 \right] \right.$$
$$\left. \times \exp\left(i\Delta k(\theta_{int}) \sum_{r=n+1}^{N} \frac{d_r}{\cos(\theta_{int})} \right) \right\}, \quad (1)$$

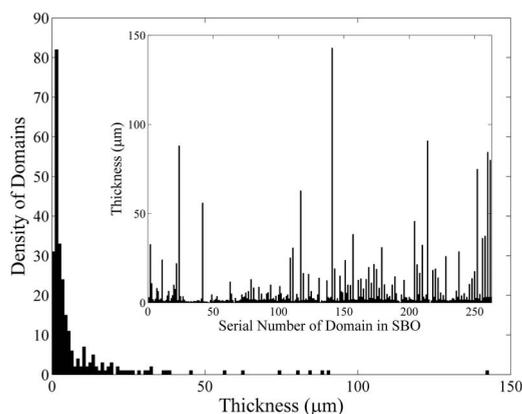where d_n is the thickness of the nth domain, $\chi_n^{(2)}$

FIG. 2. Density of domains as a function of domain size in the sample of SBO crystal under study. Inset: the thickness of domains as the function of domain number.
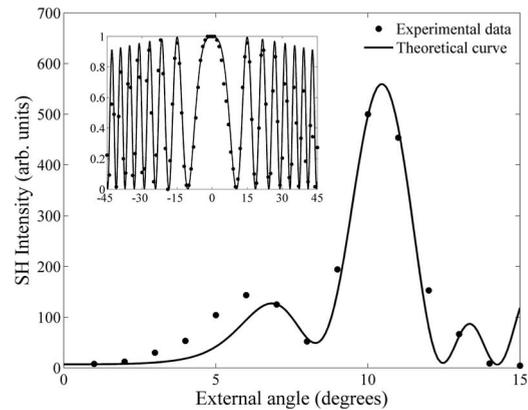

FIG. 3. Angular dependence of second-harmonic generation due to RQPM. Inset: Maker fringes in a single-domain sample of SBO. Both vertical scales are normalized to the maximum signal of Maker fringes.

$= (-1)^n |\chi^{(2)}|$ accounts for the opposite sign of nonlinear susceptibility in alternate oppositely poled domains, N is the full number of domains, θ_{int} is internal angle of propagation, and $\Delta k(\theta_{int})$ is the wave-vector mismatch with account of the anisotropy of the refraction index. This formula is easily obtainable from those used in [6,7] via the change of domain thickness in the direction perpendicular to the domain walls by the path length of the light propagating at the internal incidence angle θ_{int} onto the domain wall. For the domain-structured crystal with spatial homogeneity of the linear refraction index the correction for reflections and angular dependence of refractive indices and effective nonlinear susceptibility can be done using an envelope function for the crystals belonging to the *mm*2 point group derived in [16]. The crystal sample used in the experiment had dimensions of 5 mm along the *a* axis, 11 mm along the *b* axis, and 9 mm along the *c* axis (according to commonly used nonstandard space-group classification of SBO as *Pnm*2$_1$). The domain structure was revealed by etching and geometrically characterized via optical microscopy. A part of the domain structure is presented in Fig. 1. This is the only place in the crystal where a part of the domains disappears on the (001) facet. All the rest of the domains protrude from one to another edge of the sample. The overall thickness of the domain structure is 2 mm. The structure contains 262 domains with thickness from tens to tenths of μm. The mean value of the domain thickness is 8 μm, while the overall standard deviation is 4 μm. The thickness of domains in accordance with their position in the structure is presented in the inset of Fig. 2. Domains with thickness smaller than 0.5 μm could not be definitely identified and measured via optical microscopy. The domain structure observed in the sample for investigation is rather typical for crystal growth of SBO. Our structure is randomized much more strongly than structures generated in numerical calculations [7]. Subtracting an even number of coherence lengths from the thickness of large domains can formally reduce it for further calculations. However, this reduction can be done only for fixed wavelength and angle. The single-crystalline part of the sample that does not contain domains can be ignored in calculations in the case where the enhancement factor due to RQPM is large enough, be-
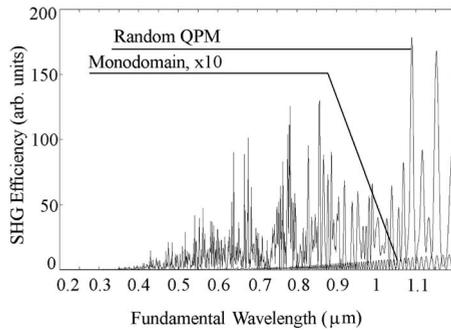
FIG. 4. Calculated spectral dependence of the second harmonic due to RQPM as a function of fundamental wavelength.

cause Maker fringes produced by it must have a much smaller oscillation amplitude. Refractive indices for calculation are taken from [17]. The linear optical homogeneity of the sample was verified via linear diffraction of helium neon laser radiation propagating along the b-axis direction. No signs of linear diffraction were detected, which means that the refractive index of neighbor domains is just the same and domain walls are very thin for SBO. The fundamental wave was the frequency-doubled Nd:YAG radiation at 532 nm with pulse energy up to 3 mJ and pulse duration 15 ns. Divergence of the beam was 3 mrad. Radiation propagated in the ab plane of the crystal so that zero angle corresponds to the direction of the a axis. Polarization of the fundamental wave was along the c axis, so that the maximal component of the nonlinear susceptibility d_{33} was employed. The rotation axis coincided with the c axis of the crystal. For these conditions $\Delta k(\theta)$ in (1) becomes independent of θ. The generated second harmonic at 266 nm was filtered with a monochromator and detected with a Hamamatsu H5773 photomultiplier module. Polarization of 266 nm radiation was verified to coincide with the c axis. Figure 3 depicts the angular dependence of RQPM. A theoretical curve calculated using (1) is fitted to experimental points by adjusting the value of Δk. The calculated curve is very sensitive to the variation of Δk in the range of 0.1%. The best fit is obtained for $\Delta k = 1.0035 \Delta k_{calc}$. The coincidence between experiment and theory is rather satisfactory up to external incidence angles of order 20°. The slight misfit in the angular position of the first maximum must be attributed to a small deviation of the observed etched domain pattern from the real domain structure. The role of the uncertainty in the domain thickness measurement increases at larger angles and leads to a larger discrepancy in the range above 20°.

Nonlinear diffraction, generally speaking, can have a certain contribution to the dependence depicted in Fig. 3. When the fundamental wave propagates at a small angle to the direction of RSV, a noncollinear interaction that involves RSV must result in the generation of an additional second-harmonic wave [18] that does not coincide with the direction of the RQPM second-harmonic wave. We checked the position of the 266-nm spot with respect to the 532-nm radiation spot and found that the former is slightly shifted to a direction opposite to the rotation direction. However, this shift is fairly explained by the difference of refractive indices that must affect the directions of the harmonic and fundamental
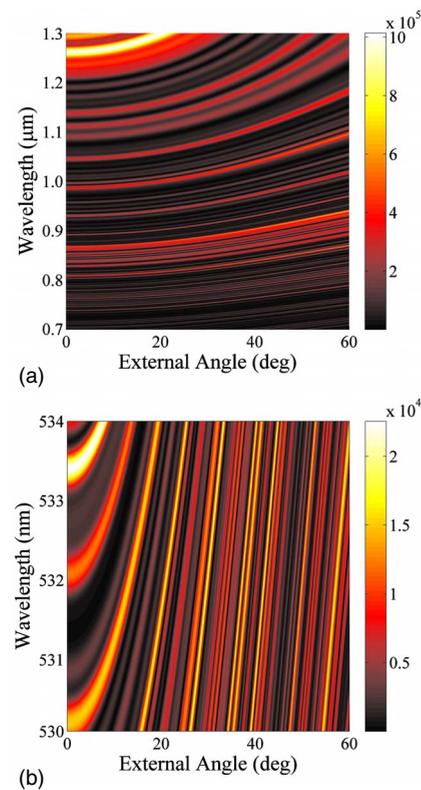

FIG. 5. (Color online) Band structure of randomized nonlinear photonic crystal sample under study (a) in the region of highest generated intensity and (b) in the vicinity of the fundamental 532 nm wavelength (calculated wave mismatch used).

after refraction of two collinear waves on the exit facet of the crystal. On the other hand, RSV values contributing to nonlinear diffraction are larger than the value K_0 necessary for QPM in the direction of the a axis, while in the case of RQPM rotating the crystal off zero incidence angle leads to employing RSV values smaller than K_0. In view of this, for domain structures with necessary statistics and most probable domain size larger than the coherence length one must expect that the contribution of RQPM will be larger than the contribution from nonlinear diffraction. For our domain structure the domain histogram is not smooth and the statistics is not large enough, and these considerations cannot be straightly applied to it. Examination of the calculated RSV spectrum of the domain structure indicates that there is a decrease of the Fourier amplitude for RSV values corresponding to domain thicknesses lower than the coherence length (in the range from 2.5 to 2.48 μm). However, the angular dependence cannot be explained by the RSV spectrum in the area above the coherence length. So the final piece of evidence for domination of RQPM is the fair agreement of experiment and calculation in Fig. 3.

The enhancement factor due to RQPM was measured by comparing the intensity at 266 nm from a domain-structured sample and from a 432-μm-thick (171 coherence lengths) reference single-domain sample of the same orientation. The latter exhibited standard Maker fringes as shown in the inset of Fig. 3. The amplitude of the central maximum of Maker fringes does not depend on the thickness of the reference

sample, but is determined by the intensity generated at one coherence length, so the reference sample thickness must not be equal to the thickness of the nonlinear photonic crystal sample. The ratio of 266 nm power from the domain structure in the second maximum at 10° to the 0° maximum of the Maker fringes pattern from a single-domain sample corrected by the ratio of envelope function values at corresponding angles gives a RQPM enhancement factor $F_{RQPM}=501$. Our calculations predict the value of $F_{RQPM}=500$. Since the coherence length for our conversion scheme is 2.526 μm and the average value of the domain thickness is 8 μm, it is clear that F_{RQPM} can be even more enhanced if the structure with smaller domains could be grown. The spectral dependence of second-harmonic intensity as a function of fundamental wavelength was calculated for the sample under investigation using (1) and is presented in Fig. 4. It consists of a number of peaks from near infrared to near ultraviolet. Maximum second-harmonic power due to RQPM is expected for the fundamental wave in the near infrared, while maximum enhancement factors are attained for the fundamental wave in the near UV. For doubling of 355 nm radiation the calculated enhancement factor for the sample under study is 2700 and the bandwidth of the peak at this wavelength is of order of 100 GHz. In analogy with the concept of the band structure of linear photonic crystal, the band structure of nonlinear photonic crystal can be introduced. It can be composed from a combination of angular and spectral dependences of nonlinearly generated radiation. For linear photonic crystal the band structure is plotted in coordinates (ω, k) and depicts the separation of the coordinate plane into areas with real and complex effective propagation vector. For nonlinear photonic crystal it is whether the same coordinates or natural coordinates like (λ, θ_{ext}) can be used. Figure 5 depicts the band structure for the randomized nonlinear photonic crystal sample studied in our paper in the latter (natural) coordinates. This band structure depicts the areas of efficient nonlinear generation in a nonlinear photonic crystal, the efficiency being plotted along the vertical axis. The band structure plot of the randomized nonlinear photonic crystal can be useful in the fitting of angular dependences of RQPM. Note that the band positions in nonlinear photonic crystal experience a rotational redshift (Fig. 5), while the band positions in randomized linear photonic crystal with nonlinear layers experience a blueshift [19]. This difference can be easily explained. Really, band positions in linear photonic crystal are determined by the variation of phase of the interfering reflected beams—namely, $kd\cos(\theta_{ext})$ [20]. As $\cos(\theta_{ext})$ decreases, one must decrease the wavelength to keep the localized mode of the fundamental radiation at the same intensity and to preserve the intensity of the generated wave. In the case of randomized nonlinear photonic crystal one must keep the constant value of $\frac{\Delta k(\theta_{int})}{\cos(\theta_{int})}$ in order to follow the position of the band maximum. Hence, a decrease of $\cos(\theta_{int})$ must be compensated by an increase of wavelength.

[1] J. A. Armstrong, N. Bloembergen, J. Ducuing, and P. S. Pershan, Phys. Rev. **127**, 1918 (1962).

[2] V. Berger, Phys. Rev. Lett. **81**, 4136 (1998).

[3] A. B. U'Ren, R. K. Erdmann, M. de la Cruz-Gutierrez, and I. A. Walmsley, Phys. Rev. Lett. **97**, 223602 (2006).

[4] S. E. Harris, Phys. Rev. Lett. **98**, 063602 (2007).

[5] E. Yu. Morozov, A. A. Kaminski, A. S. Chirkin, and D. B. Yusupov, Pis'ma Zh. Eksp. Teor. Fiz. **73**, 731 (2001) [JETP Lett. **73**, 647 (2001)].

[6] M. Baudrier-Raybaut, R. Haïdar, Ph. Kupecek, Ph. Lemasson, and E. Rosencher, Nature (London) **432**, 374 (2004).

[7] X. Vidal and J. Martorell, Phys. Rev. Lett. **97**, 013902 (2006).

[8] A. Bahabad, N. Voloch, A. Arie, A. Bruner, and D. Eger, Phys. Rev. Lett. **98**, 205501 (2007).

[9] G. Kh. Kitaeva, Phys. Rev. A **76**, 043841 (2007).

[10] A. S. Aleksandrovsky, A. M. Vyunishev, A. I. Zaitsev, A. V. Zamkov, and V. G. Arkhipkin, J. Opt. A, Pure Appl. Opt. **9**, S334 (2007).

[11] A. R. Tunyagi, M. Ulex, and K. Betzler, Phys. Rev. Lett. **90**, 243901 (2003).

[12] Y. LeGrand, D. Rouede, C. Odin, R. Aubri, and S. Mattauch, Opt. Commun. **200**, 249 (2001).

[13] A. L. Aleksandrovskii and V. V. Volkov, Kvantovaya Elektron. (Moscow) **23**, 557 (1996) [Quantum Electron. **26**, 542 (1996)].

[14] A. I. Zaitsev, A. S. Aleksandrovsky, A. D. Vasiliev, and A. V. Zamkov, J. Cryst. Growth **310**, 1 (2008).

[15] V. Petrov, F. Noack, Dezhong Shen, Feng Pan, Guangqui Shen, Xiaoqing Wang, R. Komatsu, and V. Alex, Opt. Lett. **29**, 373 (2004).

[16] P. S. Bechthold and S. Haussuhl, Appl. Phys. **14**, 403 (1977).

[17] Yu. S. Oseledchik, A. I. Prosvirnin, V. V. Starshenko, V. Osadchuk, A. I. Pisarevsky, S. P. Belokrys, A. S. Korol, N. V. Svitanko, S. A. Krikunov, and A. F. Selevich, Opt. Mater. (Amsterdam, Neth.) **4**, 669 (1995).

[18] M. M. Fejer, G. A. Magel, D. H. Jundt, and R. L. Byer, IEEE J. Quantum Electron. **28**, 2631 (1992).

[19] M. Centini, D. Felbacq, D. S. Wiersma, C. Sibilia, M. Scalora, and M. Bertolotti, J. Eur. Opt. Soc. Rapid Publ. **1**, 06021 (2006).

[20] M. Born and E. Wolf, *Principles of Optics* (Pergamon, New York, 1964), Sec. 7.5.